Journal of Optoelectronics and Advanced Materials Vol. 5, No. 2, June 2003, p. 511 - 520

THIN BARIUM LAYER FORMATION AND ITS INFLUENCE ON TUNGSTEN ELECTRODE ARC ATTACHMENT MODES IN *HID* LAMPS

M. Cristea*, G. Zissis[a]

"Politehnica" University of Bucharest, Physics Department, Splaiul Independentei 313, 77206 Bucharest, Romania
[a]Paul Sabatier University of Toulouse, Centre for Plasma Physics and Applications of Toulouse, Route de Narbonne 118, Toulouse, France

In this paper the influence of electric field, voltage drop and Schottky corrected work function on thin barium monolayer regarding the diffuse or hot-spot formation in the refractory cathode are analysed. Using the thermal flux continuity equation the hot-spot dimension is calculated. Based on the energy balance equation, a 3D model for getting the temperature distribution in the bulk of high-intensity discharge lamp electrodes operating in hot-spot mode is presented. In this case the electrode life-time is drastically reduced by the barium layer consumption and consequently by the local temperature increase and tungsten erosion.

(Received March 25, 2003; accepted May 8, 2003)

Keywords: Barium doped tungsten, Thin layer, Work function reduction, Diffuse and hot-spot mode functioning.

1. Introduction

The most important elements of high intensity discharge (HID) lamps are the electrode design and materials. The lamp life-time, the walls blackening and the functioning stability are determinated by the cathode. For the most types of HID lamps, a high intensity current is required. To satisfy this condition the electrode material must have a high melting point, a low vapour pressure, a good shape stability and a high chemical and micro-structural stability. The most used electrode materials are pure tungsten, thoried tungsten or barium doped tungsten. These materials have a good electron emissivity when their temperature is in 1500 K - 2300 K range.

Recently, an increasing interest for arc-electrode interaction modelling is observed. This is determined on one hand by the necessity for a good understanding of the complex mechanism governing the plasma-electrode interaction, and on the other hand, by the necessity to develop plasma devices with better performances.

The cathode spot formation is an effect of the non-linear character of the energy balance equation. So, the presence on the cathode surface of a small temperature (T) variation, makes the "electrical" ($\propto T^2$) and "optical" ($\propto T^4$) spot dimensions much smaller than the thermal gradient region. A theoretical prediction of different operating modes (diffuse or hot spot) of cathode arc attachment is given in [1]. Recently, new arc attachment modes were experimentally observed: the super-spot mode [2] and the spectroscopic blue-core mode [3].

Many authors have made theoretical models by using various simplifications. Starting from Waymouth [4], Tielemans-Oostvogels [5] and Cram [6], the analysis of the cathode operating mechanisms became more and more complicated and detailed. Theoretical [7-9], experimental and computational [10,11] studies were elaborated in the last years.

The aim of this paper is to make an analysis of external parameters influence, like electric field intensity or voltage drop, on the work function of thin barium layer, and to determine what kind

* Corresponding author: m. cristea@physics1.physics.pub.ro

of attachment mode is formed. Also, the spot radius is calculated. Using a 3D model, the thermal distribution in the electrode bulk is obtained by finite element method algorithm. The effects of different arc attachment modes on the cathode life-time are discussed.

2. The model

The cathode for HID or high-pressure sodium lamps (HPS) is made of tungsten rod over which are wrapped one or two coils layers of the same material (Fig. 1). The main geometrical characteristics of the lamp electrode used in this model are: $d_1 = 1.5$ mm, $d_2 = 5$ mm, $d_3 = 3$ mm, $r_1 = 0.5$ mm, $r_2 = 1.5$ mm and $r_3 = 1$ mm.

The role of wrapped layers is twofold: first to increase the radiant surface, and second to allow the storage of the emissive material between the coil interstitions. Usually the emissive mixtures are made of barium, calcium or thorium oxides (BaO, CaO, ThO_2) and of carbonates ($BaCO_3$, $CaCO_3$). Because of their radioactive properties, in the last time, ThO_2 is ofen replaced by Y_2O_3. Barium oxide is the most frequently used. By sinterisation Ba_3WO_6 and Ba atoms in excess are generated accordly with following reaction:

$$6BaO + W \rightarrow Ba_3WO_6 + 3Ba \tag{1}$$

The barium tungstanat Ba_3WO_6 remains localised at tungsten-mixture interface, and the barium atoms migrate at the electrode surface. The role of $CaCO_3$ and of Y_2O_3 are to increase the thermal stability of the emissive mixture. According to Bhalla [12], the mixtures based on tungstanat are more resistant at atmospherical contamination if the sinterisation is made in the presence of Y_2O_3.

By Levitskii and *col*. [13], the barium tungstanat can release barium atoms following the reaction:

$$5Ba_3WO_{6(s)} + W_{(s)} \rightarrow 6Ba_2WO_{5(s)} + 3Ba_{(g)} \tag{2}$$

where "*s*" and "*g*" symbolise the solid state respectively the gaseous state.

An important loss of emissive material is made through $Ba_{(g)}$ evaporation (resulted from reaction (2)) and through barium oxide evaporation from the reaction:

$$Ba_3WO_{6(s)} \xrightarrow{\leftarrow} Ba_2WO_{5(s)} + BaO_{(g)} \tag{3}$$

Using thermodynamically data founded in the literature, the conclusion is: Ba_3WO_6 is preferred as emissive material in the high-pressure discharge with respect to BaO, especially used in the low-pressure discharge. The Ba_3WO_6 vaporisation rate is reduced in comparison with the BaO rate.

The Ba atoms monolayer formation has the role to decrease the electron work function from 4.5eV (case of pure W) to 2.61eV (case of Ba).

In order to leave the metal, the electrons need energy to overshoot the potential barrier at the metal surface. This energy is called work function. At the absolute zero temperature, the last electron occupied level is Fermi level. By heating the metal, the electrons are drugged to energy levels higher than Fermi level. The electron energy distribution function is given by Fermi-Dirac statistics. At higher electrode temperature, more electrons in the tail of the energy distribution function have

sufficient energy to overshoot the electric potential barrier. This process is called thermionic emission [14].

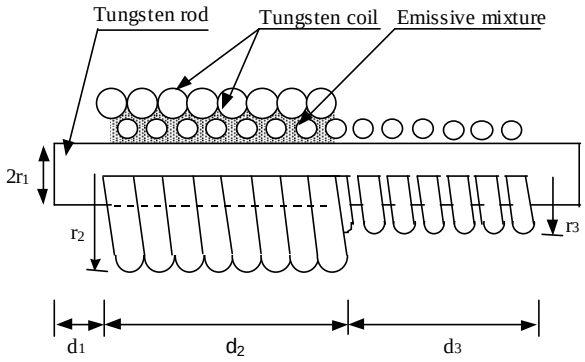

Fig. 1. Electrode of HID and HPS lamps.

In HID and HPS lamps, the electron emission is generally described by the field-enhanced thermionic emission (FEE) process using the Richardson-Duschman equation corrected by Schottky effect (j_e^{th}) [15]. The secondary emission is described by the γ-Townsed process ($j_e^{\sec}$). Using the β-Waymouth coefficient which gives a relation between ionic (j_i) and electronic (j_e) current density in the cathode neighbouring [4], we obtain:

$$j_e^{th} = AT^2 \exp\left(-\frac{e\varphi}{k_B T}\right) \; ; \quad \varphi = \varphi_0 - \Delta\varphi \quad ; \; \Delta\varphi = \left(\frac{eE_k}{4\pi\varepsilon_0}\right)^{1/2} \tag{4}$$

$$j_e^{\sec} = \gamma j_i \tag{5}$$

$$\beta = \frac{j_i}{j_e} = \frac{j_i}{j_e^{th} + j_e^{\sec}} \tag{6}$$

Here, $A = 4\pi e m_e k_B^2 / h^3 = 1.2\times10^6$ $\mathrm{Am^{-2}K^{-2}}$ represents the Richardson-Duschman constant, φ_0 is the work function of the electrode material, $\Delta\varphi$ is the Schottky correction of work function. Also, e and m_e represent the electron charge and mass respectively, k_B is Boltzmann constant, h is Planck constant and E_k is the electric field intensity in the cathode fall.

Considering that the local discharge current density in the emissive spot area is $j = j_e + j_i$, we set the following equation:

$$\frac{1-\beta\gamma}{1+\beta}\cdot\frac{h^3}{4\pi e m_e k_B^2}\cdot j = T^2 \exp\left(-\frac{e\varphi_0}{k_B T}\right)\exp\left[\frac{e^{3/2}E_k^{1/2}}{\left(4\pi\varepsilon_0\right)^{1/2} k_B T}\right] \tag{7}$$

This equation shows dependence between electrode temperature in the emissive area T, discharge current density j, β-Waymouth and γ-Townsed coefficients, work function φ_0 and electric field intensity at the cathode surface E_k.

The cathode fall field, E_k, is related to the potential drop over the free fall sheath, V_k, by MacKeon equation [16]:

$$E_k^2 \approx \frac{4j_i}{\varepsilon_0}\left(\frac{m_i V_k}{2e}\right)^{1/2} \tag{8}$$

with m_i the ion (mercury or sodium) mass.

Our model is made for mercury lamps cathode with barium doped tungsten electrode, so that the value of m_i and φ_0 were taken 3.34×10^{-25} kg respectively 2.61 eV. In the electric discharge stationary regime, a relationship between electric field intensity, cathodic voltage drop and electrode surface temperature is obtained:

$$V_k T^4 - a_1\left(\frac{1-\beta\gamma}{\beta}\right)^2 E_k^4 \cdot \exp\left(\frac{b_1 - c_1 E_k^{1/2}}{T}\right) = 0 \tag{9}$$

with $a_1 = \frac{e\varepsilon_0^2}{8m_i A^2} = 3.2576\times10^{-30}$, $b_1 = \frac{2e\varphi_0}{k_B} = 6.0522\times10^4$ and $c_1 = \frac{2e^{3/2}}{k_B\sqrt{4\pi\varepsilon_0}} = 0.8796$. All constants are in IS units.

Supplementary, a condition for total discharge current must be verified:

$$I = 2\pi \int_0^{r_{spot}} jr \cdot dr \tag{10}$$

Here r_{spot} is the spot size radius and j is the current density distribution in the spot domain given by:

$$j = A\frac{1+\beta}{1-\gamma\beta}T^2 \exp\left(-\frac{e\varphi}{k_B T}\right) \tag{11}$$

The relations (9) and (10) gives the dependence $f(V_k, E_k, T) = 0$ for all the cases when the discharge cover the entire front surface of the electrode or an important fraction of it.

In this work we study the situation when the discharge area do not cover uniformly all front electrode surface. It is proved experimentally that in the spot area many zones with different brightness can appear [17]. This means that the spot is fragmented in many parts, and many micro-emissive sites corresponding to filamentary currents can be formed. This fragmentation is favorized by high-pressure values. The mutual self-magnetic interaction force between these filamentary currents has a concurrent effect. The magnetic interaction, being responsible for filaments and emissive sites merging, leads to only one emissive area. In this work, we suppose that the all current is located in a unique circular hot-spot area with radius r_{hs}.

The spatial constriction of the arc current in the spot area due to the self-magnetic force implies a high temperature in this area. Pictures taken with a long-distance microscope and a CCD camera [10] shows a smooth area in the moving regions of the hot-spot. This is caused by a local melting of tungsten. For these reasons, the hot-spot cathode temperature is supposed to be equal with tungsten melting temperature T_{hs} = 3683 K. Because of a supplementary heating due to the increase of

the ionic bombardment this temperature (T_{hs}) is not constant when the discharge pressure increases. This increase is very slow and can be neglected.

To calculate the hot-spot dimension r_{hs} at the hot-spot temperature (T_{hs}), the energetic flux conservation equation must be solved:

$$\vec{q}_1 + \vec{q}_2 + \vec{q}_3 + \vec{q}_4 + \vec{q}_5 = 0 \tag{12}$$

The scalar projections of the above equation terms and their significance are:

- $q_1 = k_w\left(T_{hs}\right)\left(\frac{\partial T}{\partial z}\right)_{z=z_{hs}}$ is the flux transported by thermal conduction toward inside of the cathode. The quantity $k_w\left(T_{hs}\right)$ is the tungsten thermal conductivity at T_{hs} temperature. $\left(\frac{\partial T}{\partial z}\right)$ represent the temperature derivative in the electrode longitudinal direction.

- $q_2 = j_i\left[V_k + V_i - \varphi\right]$ is the energetic flux transported by the ions. Here V_i is the ionisation potential and φ is the work function.

- $q_3 = j_e\left[\varphi + \frac{2k_B T_{hs}}{e}\right]$ is the energetic flux lost by the cathode due to the emitted electrons (Nottingham effect).

- $q_4 = \sigma\varepsilon_w\left(T_{hs}\right)T_{hs}^4$ is the outward radiative flux from the cathode spot, where σ is Sefan-Boltzmann constant and $\varepsilon_w\left(T_{hs}\right)$ is the total tungsten emissivity at T_{hs} temperature.

- $q_5 = \sigma\varepsilon_w\left(T_{hs}\right)T_{plasma}^4$ is the radiative energetic flux absorbed in the electrode and arriving from the plasma. The central discharge plasma temperature does not depend sensitively on the discharge current (experimentally proved), and for this reason we consider $T_{plasma} = 5800K$.

In equation (12), we neglect the heat exchange between plasma and cathode due to conduction. This is justified by the fact that in the free-fall sheath zone the matter is almost absent and, consequently, the energetic exchange by collisions is very low.

Considering that all current intensity I is passing through the circular spot area with radius r_{hs} and using the β Waymouth coefficient, we obtain:

$$\frac{I}{\pi r_{hs}^2(1+\beta)}\left[\beta\left(V_k + V_i\right) - \varphi(1+\beta) - \frac{2k_B T_{hs}}{e}\right] - \sigma\varepsilon_w\left(T_{hs}\right)\left[T_{hs}^4 - T_{plasma}^4\right] = k_w\left(T_{hs}\right)\left(\frac{\partial T}{\partial z}\right)_{z=z_{spot}} \tag{13}$$

which allows the calculation of the hot-spot radius dependence on the discharge current discharge.

To obtain the temperature distribution in the cathode bulk material, the heat transport equation must be solved

$$\rho c\frac{\partial T}{\partial t} = \nabla\left[-k_w(T)\nabla T\right] + S \tag{14}$$

where $\rho = 19300kg/m^3$ is the tungsten density, $c = 132J/kg/K$ is the tungsten heat capacity, and S is the source term given by Joule effect $S = \rho_e j^2$, with ρ_e is the electric resistivity of the electrode.

The heat produced in the electrode material by the discharge current increase the temperature, and the tungsten electric conductivity is changing. The change is given by the relation:

$$\rho_e(T) = \rho_{0e}\left[1 + \alpha\left(T - T_0\right)\right] \tag{15}$$

where $\rho_{0e} = 4.312 \times 10^{-8}\,\Omega m$ and $\alpha = 6.76 \times 10^{-3} K^{-1}$ are the resistivity at $273.15\,K$ and the thermal resistivity coefficient, respectively.

In order to solve the partial differential equation (14), we need to know the boundary conditions. These are presented as follows:

The hot-spot domain and the end part of the electrode are characterised by Dirichlet boundary conditions: $T = T_{hs}$ and $T_{end} = 600K$. A Neumann boundary condition like in [18, 19] references was imposed for the rest of the frontier:

$$\vec{n} k_w \left(\frac{\partial T}{\partial \vec{n}}\right)_b = \vec{n}\left[\varepsilon_w\left(T_b\right)\sigma\left(T_b^4 - T_{amb}^4\right) + \zeta\left(T_b - T_{amb}\right)\right] \tag{16}$$

where T_b represent the border temperature, ζ is the convection transport coefficient and $\left(\frac{\partial T}{\partial \vec{n}}\right)_b$ represent the temperature derivative in the normal direction ($\vec{n}$) of the cathode surface. The ambient temperature T_{amb} is considered equal at $300\,K$, and for the convection transport coefficient we take $\zeta = 25\,Wm^{-2}K^{-1}$. The temperature dependence of tungsten thermal conductivity and emissivity are the analytical functions, which fit the literature data [20]:

$$k_w(T) = \frac{776}{T^{0.256}} \tag{17}$$

$$\varepsilon_w(T) = -5.6148 \times 10^{-2} + 1.6019 \times 10^{-4} \times T - 1.3685 \times 10^{-8} \times T^2 \tag{18}$$

All the coefficients are given in IS units.

The above equations describing the system have been solved in steady state by using a finite element method, based on FEMLAB software.

3. Results and discussions

Some of the results obtained by numerical simulation are presented below. In Fig. 2, the voltage drop dependence of the cathode electric field intensity is presented for various values of electrode spot temperature when β-Waymouth and γ-Townsend coefficients are equal to 0.1 and 0.01 respectively.

It can be clearly seen that for given discharge current and voltage drop, two operating modes are possible: the first, when the field intensity is lower (case of "diffuse" mode operation), and the second one, when the field intensity is higher of $E > 10^8 V/m$ (case of "hot-spot" mode).

This bifurcation behaviour can be explained by the work function modification through Schottky correction. The voltage drop dependency of work function for a thin barium layer on the tungsten electrode surface is presented in Fig. 3.

At the same voltage drop, when the electric field intensity is relatively low, the work function remains approximately constant for a large voltage range. In this case, the entire cathode surface participates at the FEE emission, and the cathode is in diffuse mode operation.

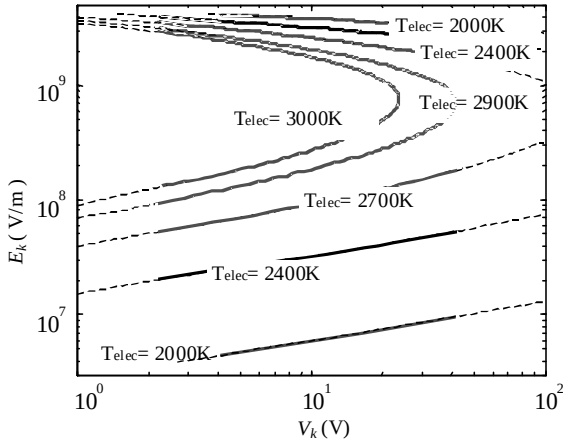

Fig. 2. Voltage drop dependence on the cathode electric field intensity.

If the field intensity is high, the work function is dramatically reduced. In order to assure a constant electrode current the electron emissive zone is diminishing (this is hot-spot mode).

In Fig. 4 the electric field dependencies of the spot radius are presented in the case of various electrode emissive zone temperatures, T_{elec}. It can be seen that if the emissive zone temperature is high (towards the tungsten melting point, 3683K), the radius dependence is very slow and have a low value. Contrary, if the emissive zone temperature is around 2000K, when the electric field intensity decreases the spot radius increases and at low field the discharge cover all cathode surface. The transition from hot-spot to diffuse mode is produced. Due to the uniform temperature distribution on all emissive surface and the relatively low value (T_{elec}), the barium vaporisation process from the monolayer have a small rate. This fact increases the electrode life-time.

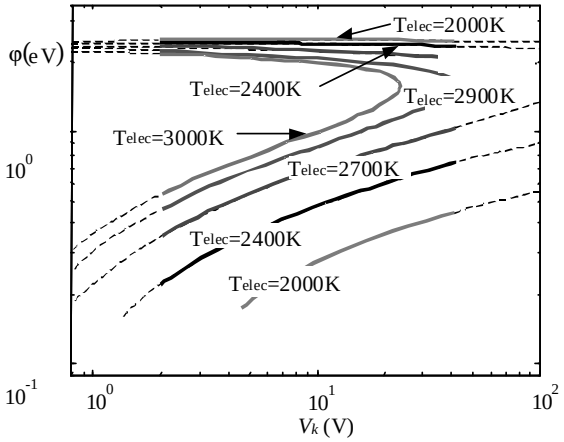

Fig. 3. Work function versus cathode voltage drop for a thin barium layer on the tungsten refractory cathode.

During the hot-spot mode working, a contrary effect with respect the electric field on the work function appears. From the theoretical point of view, the work function value is determined by the dopant coverage fraction degree in the spot area. This degree varies during the working by barium atoms desorption, re-adsorption and diffusion processes through the tungsten matrix. When the emissive size area diminish, the current density increase corespondent in order to assure a constant discharge current. Now, the electrode temperature increase by Joule effect. A high local temperature

of the electrode make a barium atoms vaporisation from the thin layer and diminish also the re-adsorption process. The work function increase and a supplementary local heating is required to assure the same current. The work function is supplementary increased by this new heating. This process is repeated more and more quickly until the barium coverage fraction became zero. The local temperature increase to the tungsten melting point. The electrode errosion by vaporization became important, and consequently the catode life-time is ending.

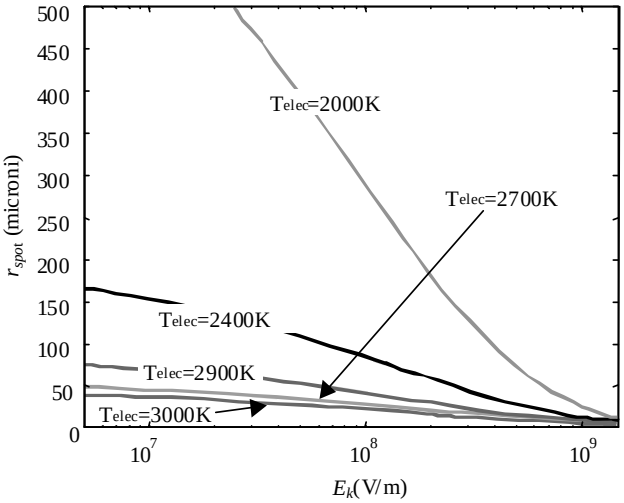

Fig. 4. Electric field dependence of spot radius at various emissive electrodes surface temperatures.

It is clear that the φ_0 value of change in every functioning moments. Casado and Colomer [21] shown that a small cathode cooling temperature increment significantly increasse the cathode life-time. Consequently, is important to know the temperature distribution in the cathode bulk.

To obtain the temperature distribution in the bulk electrode material, the heat transport equation (14) with mixed boundary conditions is solved by using FEMLAB software. The calculations are made for $2.5\,A$ intensity current discharge. The spot domain is supposed to be circular with radius given by temperature dependence from Fig. 4. The spot is localised in an arbitrary point of active electrode surface (0.3 mm distance from symmetry axis). In Fig. 5a) a integral view of the cathode temperature distribution is shown while Fig. 5b) present this distribution in a middle longitudinal cathode section passing from the hot-spot. In Fig. 5c) and 5d) are presented a hot-spot region detailed pictures.

The hot-spot arc attachment area is located nearby the cathode edge corresponding to the high electric field place. This localisation is also due to the construction defects, non-homogeneities, roughness of material and lower thermal conduction inside the cathode. This fact allows the local temperature increasing and consequently, a high electron emission leads to an additional heating by Joule effect. The electrode material can rapidly reach its melting point. Then, the material locall evaporation is very rapid. This process can be assimilated to an explosion. This explosion abruptly change the local electrode characteristics and consequently the hot-spot will move to another place. The hot-spot movement is also influenced by the emissive layer vaporisation. These local fluctuations being very important, the hot-spot movement direction cannot be predicted. The movement is likewise the Brownian motion [18, 22]. Dynamics of the spot movement is mainly determined by the electrode geometry. It is known that, for large diameters (1.5 – 2 mm) the hot-spot movement is very slow, and became fast for small diameters [10]. This behaviour is due to the difference in temperature between hot-spot area and remaining cathode surface.

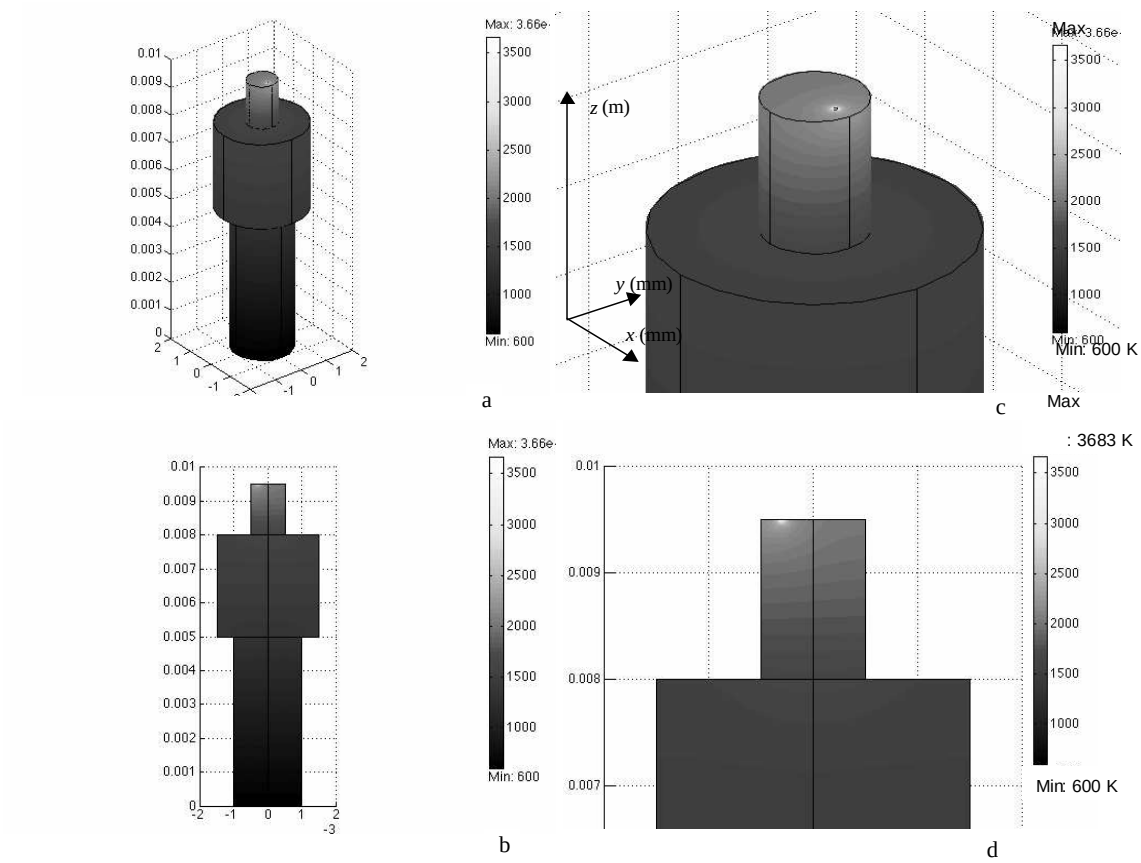

Fig. 5. Cathode temperature distribution in the electrode (a) and in the longitudinal section through the spot (b). Detail of the same distribution in the hot-spot zone (c, d).

The processes described above are more complicated because the work function is changing every moment with respect to the fraction coverage value θ. For $\theta \le 1$ the experimental dependence of the effective work function can be described by a simple relationship $\varphi(\theta) = \varphi_{\min} + (\varphi_w - \varphi_{\min})(1-\theta)^2$. The work function maximum values is $\varphi_w = 4.5$ eV coresponding to pure tungsten cathode surface ($\theta = 0$). The $\varphi_{\min}$ value depend on the tungsten substrat crystallographic characteristics.

A more complicated model can be elaborated assuming that the cathode work function is not in stationary regime. The value is changing by fraction coverage θ. This fraction depends on the electrode point temperature, diffusion, adsorption, desorbtion and re-adsorption barium atoms processes, and is not an easy thing to be done.

4. Conclusion

A study of the electric field, voltage drop and Schottky corrected work function influence on hot-spot formation in the refractory electrode was carried out. A 3D model able to obtain the temperature distribution in high-intensity discharge bulk electrode operating in hot-spot mode was presented. This model is based on the energy balance and thermal flux continuity equations. The model equations with Dirichlet and non-linear Neumann boundary conditions were solved using a FEMLAB and MATLAB software. Consequently, the developed algorithm can be exported to

SIMULINK, a very large software, in order to obtain a global model of lamp, its electrodes, and the associated power supply.

Acknowledgement

This work was partially supported by the European Project NumeLiTe (NNE 5 – 2001 – 0282) and the "Brâncusi" Franco-Roumanian Project No. 1 (I54 – 02 - 03).

References

[1] G. Ecker, Ergebnisse der Exacten Naturwissenchaften **33**, 1, 104 (1961).
[2] T. Hartman, K. Gunther, S. Lichtenberg, D. Nandelstadt, L Dabringhausen, M. Redwitz, J. Mentel, J. Phys. D: Appl. Phys. **35**, 1657 (2002).
[3] J. Reiche, F. Konemann, W. Mende, M. Kock, J. Phys. D: Appl. Phys. **34**, 3177 (2001).
[4] J. F. Waymouth, J. Light & Vis. Env. **6,** 53 (1982).
[5] P. Tielemans, F. Oostvoegels, Philips J. Res. **38** (4-5), 214 (1983).
[6] L. E. Cram, J. Phys. D: Appl. Phys. **16,** 1643 (1983).
[7] B. Juttner, J. Phys. D: Appl. Phys. **34,** R103 (2001).
[8] S. Coulombe, J-L. Meunier, J. Phys. D: Appl. Phys. **30,** 2905 (1997).
[9] M. S. Benilov, M D. Cunha, J. Phys. D: Appl. Phys. **35,** 1736 (2002).
[10] S. Lichtenberg, D. Nandelstadt, L. Dabringhausen, M. Redwitz, J. Luhmann, J. Mentel, J. Phys. D: Appl. Phys. **35,** 1648 (2002).
[11] J. Mentel, L. Dabringhausen, S. Lichtenberg, J. Luhmann, D. Nandelstadt, M. Redwitz, Proc. 9th Inter. Symp. on the Science and Technology of Light Sources, Ithaca, NY, USA, 2001, p.177.
[12] R. S. Bhalla, J. Illum. Eng. Soc, **8**, 174 (1979).
[13] V. A. Levitskii, Yu. Hekimov, Ja. I. Gerassimov, J. Chem. Thermodynamics **11**, 1075 (1979).
[14] J de Groot, J van Vliet, The high-pressure sodium lamp, Philips Technical Library, Deventer (1986).
[15] S. Coulombe, J-L. Meunier, J. Phys. D: Appl. Phys. **30,** 776 (1997).
[16] S. S. MacKeon, Phys. Rev. **95**, 611 (1929).
[17] B. Juttner, J. Phys. D: Appl. Phys. **30** 221 (1997).
[18] M. Cristea, I. Iova, I. M. Popescu, Romanian Reports in Physics **50** (10), 765 (1998).
[19] M. Cristea, I. Iova, C. P. Cristescu, I. M. Popescu, J. J. Damelincourt, Contr. Plasma Phys. **40** (5-6), 545 (2000).
[20] F. P. Incropera, D. P. de Witt, Fundamentals of Heat and Mass Transfer, John Wiley & Sons, Second edition, New-York (1985).
[21] E. Casado, V. Colomer, J. Phys. D: Appl. Phys. **33**, 1342 (2000).
[22] M. Cristea, C. Cristescu, J. J. Damelincourt, 19th SPIG (Symposium of the Physics of Ionised Gases), Zlatibor, Yugoslavia, 1998, Contributed papers, p.525.